ACADEMIC PRESS

Available online at www.sciencedirect.com

SCIENCE DIRECT®

Journal of Computational Physics 186 (2003) 122–135

JOURNAL OF COMPUTATIONAL PHYSICS

www.elsevier.com/locate/jcp

Simulation of anisotropic diffusion by means of a diffusion velocity method

A. Beaudoin, S. Huberson, E. Rivoalen *

Laboratoire de Mécanique, Fac.des. Sciences & Techniques, Université du Havre, 25 rue Philippe Lebon, BP 540, Le Havre Cedex 76058, France

Received 17 January 2002; received in revised form 23 September 2002; accepted 20 December 2002

Abstract

An alternative method to the Particle Strength Exchange method for solving the advection–diffusion equation in the general case of a non-isotropic and non-uniform diffusion is proposed. This method is an extension of the diffusion velocity method. It is shown that this extension is quite straightforward due to the explicit use of the diffusion flux in the expression of the diffusion velocity. This approach is used to simulate pollutant transport in groundwater and the results are compared to those of the PSE method presented in an earlier study by Zimmermann et al.

Keywords: Particle method; Diffusion; Dispersion

1. Introduction

In a recent paper, Zimmermann et al. [18] have explored the application of the PSE method to non-isotropic non-uniform diffusion. Although this extension of the method was derived more than ten years ago by Degond and Mas-Gallic [7], this is one of the very first attempt to use it in order to solve a physical problem, here the dispersion in groundwater flows. The work by Zimmermann et al. involves a re-griding technique previously developed by Koumoutsakos and Cottet which is fully described as well as many other interesting aspects of particle method in [6]. An alternative method for the simulation of diffusion process has been developed in the last decade, specially for external flows. It is based on the diffusion velocity concept and includes a few interesting characteristics [8,10]. Particularly, the extension of this method to non-isotropic non-uniform diffusion problems is quite straightforward which was not the case for any other existing particle methods. This is due to the fact that the diffusion flux rather than the diffusion operator is considered in these methods. In this paper, we take the opportunity offered by Zimmermann et al. work to test the method and to compare its behavior to that of the PSE method. The same test problems have been

* Corresponding author. Tel.: +33-2-32-74-49-76; fax: +33-2-32-74-49-60.
E-mail addresses: Anthony.Beaudoin@univ-lehavre.fr (A. Beaudoin), huberson@univ-lehavre.fr (S. Huberson), rivoalen@univ-lehavre.fr (E. Rivoalen).

0021-9991/03/$ - see front matter
doi:10.1016/S0021-9991(03)00024-X

used and the numerical tests have been performed with and without re-griding in order to derive an estimate of the limitation of the self-adaptivity to the method. We believe that the velocity diffusion method offers a valuable alternative at least for the particular case of dispersion problem in aquifer which was addressed in the last part of Zimmermann et al. paper.

2. Numerical model

2.1. Particle approximation of the advection–dispersion equation

The advection–dispersion equation can be written as follows:

$$\frac{\partial c(\mathbf{x},t)}{\partial t} + \mathbf{u}(\mathbf{x},t)\cdot\nabla c(\mathbf{x},t) = \nabla(\mathbf{D}(\mathbf{x},t)\cdot\nabla c(\mathbf{x},t)), \tag{1}$$

where $\mathbf{u}(\mathbf{x},t)$ is the mean velocity field, $c(\mathbf{x},t)$ is the contaminant concentration and $\mathbf{D}$ is the dynamic dispersion tensor. In this paper, we consider that the contaminant is a conservative solute. There is no mass transfer to other species or chemical reaction. Only the advection and dispersion have been simulated. As usual in particle methods, the contaminant concentration field is discretized in a set of particles $\mathscr{P}_i$. Each particle $\mathscr{P}_i$ is defined by its location $\mathbf{x}_i(t)$ and its weight $c_i(t)$. The contaminant concentration can be approximated by:

$$c_{\mathrm{h}}(\mathbf{x},t) = \sum_i c_i(t)\zeta_\varepsilon(\mathbf{x}-\mathbf{x}_i(t)), \tag{2}$$

where $c_{\mathrm{h}}(\mathbf{x},t)$ is the approximated concentration and ζ_ε is the usual smoothing function. This function is defined by $\zeta_\varepsilon(\mathbf{x}) = (1/\varepsilon^n)\zeta(\mathbf{x}/\varepsilon)$, where n is the space dimension and ε is the smoothing parameter [6]. This smoothing function satisfies the following moment conditions:

$$\int_{\mathbb{R}^2}\zeta_\varepsilon(\mathbf{x})\,\mathrm{d}x\,\mathrm{d}y = 1 \quad \text{and} \quad \int_{\mathbb{R}^2}\mathbf{x}\zeta_\varepsilon(\mathbf{x})\,\mathrm{d}x\,\mathrm{d}y = 0. \tag{3}$$

There are three main classes of algorithms to account for the dispersion term in the advection–dispersion equation. The first class is the random walk technique introduced by Chorin [4,5]. It is based on the analogy between a standard brownian motion and a diffusion process. The second class of methods is the integral approximation of the diffusion operator of the advection–diffusion equation [3,7,9]. This is the method which has been used in Zimmermann et al. work. The third class of methods uses the notion of diffusion velocity. In this third class, the diffusion term is interpreted as the displacement of particles in a direction which is aligned with the local concentration gradient. This displacement results from a diffusion velocity which is added to the advection velocity [8,17]. The existence of the solution of the modified equation as well as the convergence of the particle method for simple cases has been proved by Lions et al. [13,15,16]. This model holds for the advection–dispersion equation too since the dispersion process is usually modelised by means of a diffusion term. The resulting equation reads:

$$\frac{\partial c(\mathbf{x},t)}{\partial t} + \nabla\cdot[(\mathbf{u}(\mathbf{x},t)+\mathbf{u}_{\mathrm{d}}(\mathbf{x},t))\cdot c(\mathbf{x},t)] = 0, \tag{4}$$

where $\mathbf{u}(\mathbf{x},t)$ is the mean velocity field and $\mathbf{u}_{\mathrm{d}}(\mathbf{x},t)$ is the dispersion velocity. The dispersion velocity is readily obtained by identifying this equation with the original advection–dispersion equation:

$$\mathbf{u}_{\mathrm{d}}(\mathbf{x},t) = -\mathbf{D}(\mathbf{x},t)\frac{\nabla c(\mathbf{x},t)}{c(\mathbf{x},t)} = -\mathbf{D}(\mathbf{x},t)\nabla\log c(\mathbf{x},t). \tag{5}$$

To solve the new advection–dispersion equation, it has to be written in a Lagrangian framework yielding the discrete form:

$$\frac{\mathrm{d}\mathbf{x}_i}{\mathrm{d}t} = \mathbf{u}(\mathbf{x}_i, t) + \mathbf{u}_\mathrm{d}(\mathbf{x}_i, t), \tag{6}$$

$$\frac{\mathrm{d}c_i}{\mathrm{d}t} = 0. \tag{7}$$

This set of differential equations has been numerically solved by using a 4th order accurate Runge–Kutta scheme. It can be pointed out that the method is conservative in the sense that the sum $(\sum_i c_i)$ is constant from Eq. (7). In the present work, a second-order, two dimensional Gaussian smoothing function has been selected:

$$\zeta_\varepsilon(\mathbf{x}) = \frac{1}{\pi\varepsilon^2} \exp\left(-\frac{|\mathbf{x}|^2}{\varepsilon^2} \right). \tag{8}$$

The diffusion velocity has to be computed through the following approximation:

$$\mathbf{u}_\mathrm{d}(\mathbf{x}, t) \approx -\mathbf{D}(\mathbf{x}, t) \frac{\nabla c_\mathrm{h}(\mathbf{x}, t)}{c_\mathrm{h}(\mathbf{x}, t)}. \tag{9}$$

$\nabla c_\mathrm{h}(\mathbf{x}, t)$ is obtained by a direct differentiation of Eq. (2) as in [8,17]. Note that the dispersivity $\mathbf{D}(\mathbf{x}, t)$ is a spherical tensor in the isotropic case and a second rank symmetric tensor in the two dimensional anisotropic case. In the rest of the paper, the Scheidegger's model [2] has been chosen:

$$\mathbf{D} = \begin{pmatrix} D_{xx} & D_{xy} \\ D_{yx} & D_{yy} \end{pmatrix}, \tag{10}$$

where

$$D_{xx} = \alpha_\mathrm{L} \frac{u_x^2}{|u|} + \alpha_\mathrm{T} \frac{u_y^2}{|u|}, \tag{11}$$

$$D_{yy} = \alpha_\mathrm{T} \frac{u_x^2}{|u|} + \alpha_\mathrm{L} \frac{u_y^2}{|u|}, \tag{12}$$

$$D_{xy} = D_{yx} = (\alpha_\mathrm{L} - \alpha_\mathrm{T}) \frac{u_x u_y}{|u|}, \tag{13}$$

$$|u| = \sqrt{u_x^2 + u_y^2}, \tag{14}$$

α_L is the longitudinal dispersivity, α_T the transversal dispersivity, u_x the component of the mean velocity field in the x direction and u_y the component in the y direction.

2.2. Re-griding procedure

The particles must overlap at any time to ensure the accuracy of the numerical solution. In order to explain the basis of this overlapping condition, it is important to keep in mind that the solution has been

approximated as a sum of individual functions which are the product of the particle weight and the smoothing function. Once the cut-off parameter has been selected, these function shapes are frozen so that it is easily understood that a coarse particle repartition will yield a shaky approximation. To overcome this problem, a re-griding procedure has to be used. This process is described in the present section and was previously applied with in the particle in cell framework [14]. The re-griding consists in two steps. The first step is a projection step. At time t_0, the old particles $\mathscr{P}_i^0$ are located at $\mathbf{x}_i^0$ and their weights are c_i^0. A regular square grid is superimposed to the domain covered by the particles. The location of new particles $\mathscr{P}_i^1$ is set on the grid node. The grid path h is the same for all directions and has been selected in order to satisfy the overlapping condition. Using the new particles, the contaminant concentration at location $\mathbf{x}_i^1$ can be calculated as:

$$c_{\mathrm{h}}^0(\mathbf{x}_i^1) = \sum_{j=1}^{N_{\mathrm{p}}^0} c_j^0 \zeta_\varepsilon(\mathbf{x}_i^1 - \mathbf{x}_j^0), \tag{15}$$

where N_{p}^0 is the old particles number. To evaluate the weight c_i^1 for each new particle $\mathscr{P}_i^1$, the following approximation can be used:

$$c_i^1 = \int_{\mathscr{P}_i^1} c_{\mathrm{h}}^0(\mathbf{x}_i^1)\,\mathrm{d}x\,\mathrm{d}y \approx h^2 c_{\mathrm{h}}^0(\mathbf{x}_i^1). \tag{16}$$

However this first step, which is something like a double projection step, introduces diffusion errors which have to be corrected. This is the goal of the second step. Two different evaluations for the projection error can be derived:

$$Er_1 = \left\| \sum_{j=1}^{N_{\mathrm{p}}^1} c_j^1 \zeta_\varepsilon(\mathbf{x}_i^0 - \mathbf{x}_j^1) - c_{\mathrm{h}}^0(\mathbf{x}_i^0) \right\|^2_{L^2(\mathbb{R}^2)}, \tag{17}$$

$$Er_2 = \left\| \sum_{j=1}^{N_{\mathrm{p}}^1} c_j^1 \zeta_\varepsilon(\mathbf{x}_i^1 - \mathbf{x}_j^1) - c_{\mathrm{h}}^0(\mathbf{x}_i^1) \right\|^2_{L^2(\mathbb{R}^2)}, \tag{18}$$

where N_{p}^1 is the new particles number. The correction procedure has been derived as a correction to be added to the weights c_i^1 of new particles $\mathscr{P}_i^1$. This correction has been computed by assuming that a good estimate for the error is provided by the product of the Laplacian of the approximated concentration $c_{\mathrm{h}}^0(\mathbf{x}_i^1)$ and a constant K. This assumption has been used to compute the correction itself. It is actually an anti-diffusion process defined as:

$$c_{ci}^1 = c_i^1 - Kh^2 \Delta c_{\mathrm{h}}^0(\mathbf{x}_i^1), \tag{19}$$

where c_{ci}^1 is the corrected value for c_i^1. To simplify the procedure, a uniform value has been retained for K. This value has been selected in order to minimize a combination of the two previously defined errors:

$$\begin{aligned} Er_1 + Er_2 = &\left\| \sum_{j}^{N_{\mathrm{p}}^1} (c_j^1 - Kh^2 \Delta c_{\mathrm{h}}^0(\mathbf{x}_j^1)) \zeta_\varepsilon(\mathbf{x}_i^0 - \mathbf{x}_j^1) - c_{\mathrm{h}}^0(\mathbf{x}_i^0) \right\|^2 \\ &+ \left\| \sum_{j}^{N_{\mathrm{p}}^1} (c_j^1 - Kh^2 \Delta c_{\mathrm{h}}^0(\mathbf{x}_j^1)) \zeta_\varepsilon(\mathbf{x}_i^1 - \mathbf{x}_j^1) - c_{\mathrm{h}}^0(\mathbf{x}_i^1) \right\|^2, \end{aligned} \tag{20}$$

this expression is a quadratic form $\alpha K^2 + \beta K + \gamma$ which is minimum for:

$$K = -\frac{\beta}{2\alpha}, \tag{21}$$

where

$$\beta = 2\left(\sum_j^{N_\mathrm{p}^0}\left(c_\mathrm{h}^0(\mathbf{x}_j^0) - \sum_i^{N_\mathrm{p}^1} c_i^1\zeta_\varepsilon(\mathbf{x}_j^0 - \mathbf{x}_i^1)\right)\sum_i^{N_\mathrm{p}^1}\Delta c_\mathrm{h}^0(\mathbf{x}_i^1)h^2\zeta_\varepsilon(\mathbf{x}_j^0 - \mathbf{x}_i^1)\right.$$
$$\left. + \sum_j^{N_\mathrm{p}^1}\left(c_\mathrm{h}^0(\mathbf{x}_j^1) - \sum_i^{N_\mathrm{p}^1} c_i^1\zeta_\varepsilon(\mathbf{x}_j^1 - \mathbf{x}_i^1)\right)\sum_i^{N_\mathrm{p}^1}\Delta c_\mathrm{h}^0(\mathbf{x}_i^1)h^2\zeta_\varepsilon(\mathbf{x}_j^1 - \mathbf{x}_i^1)\right), \tag{22}$$

$$\alpha = \sum_j^{N_\mathrm{p}^0}\left(\sum_i^{N_\mathrm{p}^1} h^2\Delta c_\mathrm{h}^0(\mathbf{x}_i^1)\zeta_\varepsilon(\mathbf{x}_j^0 - \mathbf{x}_i^1)\right)^2 + \sum_j^{N_\mathrm{p}^1}\left(\sum_i^{N_\mathrm{p}^1} h^2\Delta c_\mathrm{h}^0(\mathbf{x}_i^1)\zeta_\varepsilon(\mathbf{x}_j^1 - \mathbf{x}_i^1)\right)^2, \tag{23}$$

A simple second order centered finite difference scheme has been used to estimate $\Delta c_\mathrm{h}^0(\mathbf{x}_i^1)$.

3. Numerical tests

3.1. Test case definition

In this section, the diffusion velocity method will be tested by comparing the numerical results obtained with this method with Zimmermann et al. [18] numerical results. Therefore the same problems have been considered and the results are presented in the same dimensional form. The contaminant was assumed to be injected at a point source in an unbounded domain where the mean velocity field has been taken uniform and constant. The source of the contaminant was located at point $\mathbf{x}(-100, 100)$. For this simple problem, an analytical solution for the concentration c_a can be derived:

$$c_\mathrm{a}(\mathbf{x}, t) = \frac{\delta M}{2\pi m n_\mathrm{e}}\frac{\exp(A)}{\sqrt{4t^2(D_{xx}D_{yy} - D_{xy}^2) + \varepsilon_\mathrm{src}^4 + 2\varepsilon_\mathrm{src}^2 t(D_{xx} + D_{yy})}}, \tag{24}$$

where

$$A = \frac{-x_t^2(2tD_{yy} + \varepsilon_\mathrm{src}^2) - y_t^2(2tD_{xx} + \varepsilon_\mathrm{src}^2) + x_t y_t 4tD_{xy}}{8t^2(D_{xx}D_{yy} - D_{xy}^2) + 2\varepsilon_\mathrm{src}^4 + 4\varepsilon_\mathrm{src}^2 t(D_{xx} + D_{yy})}, \tag{25}$$

$$x_t = x - u_x t \quad \text{and} \quad y_t = y - v_y t, \tag{26}$$

δM is the mass of injected pollutant, m is the thickness of the aquifer, n_e is the effective porosity and ε_src is the width of the Gaussian initial concentration. This analytical solution has been extensively used to check the accuracy of the diffusion velocity method. As in Zimmermann et al. work, the validation study consists in four tests. For each test, only one parameter has been varied: the smoothing parameter ε, the time step δt, the re-griding frequency N_f and the dispersion ratio α. For each case, the numerical parameters used are given in Table 1. The computer code was a very crude version of the $\mathcal{O}(N_\mathrm{p}^2)$ summation method which has been parallelised for a 32 Beowulf CPU cluster. Therefore, the CPU time of the simulations is by no way

Table 1
Parameters used for the validation study (m, n_e, ε_{src} and h/ε are fixed for all cases)

Case	u_x (m/d)	u_y (m/d)	α_L (m)	α_T (m)	β (degrees)	δm (g)	N_t	δt (days)	N_f	ε (m)
1	1.0	0.0	10.0	1.0	0.0	125,000	4–100	2–50	10	7–14
2	$\frac{\sqrt{2}}{2}$	$-\frac{\sqrt{2}}{2}$	10.0	1.0	−45.0	125,000	100–250	2	10	7–14
3	1.0	0.0	100.0	10.0	0.0	125,000	20–400	0.5–10	10	11
4	$\frac{\sqrt{2}}{2}$	$-\frac{\sqrt{2}}{2}$	100.0	10.0	−45.0	125,000	20–400	0.5–10	10	11
5	0.6	−0.8	10.0	1.0	−53.0	125,000	100	2	10	7–14
6	$\frac{\sqrt{2}}{2}$	$-\frac{\sqrt{2}}{2}$	0.0	0.0	−45.0	1,000,000	30	10	1	11
7	$\frac{\sqrt{2}}{2}$	$-\frac{\sqrt{2}}{2}$	100.0	1.0	−45.0	1,000,000	100–10,000	2	1–10	11

m (m)	n_e	ε_{src} (m)	h/ε
7.0	0.37	44.0	0.9

comparable to the results obtained by Zimmermann et al. with a fully optimized method. The use of a fast multipole solver [1,11] is obviously highly desirable although it remains to be implemented.

3.2. Smoothing parameter ε

In order to check the influence of the smoothing parameter ε on the numerical results, three cases denoted 1, 2 and 5 have been considered (see Table 1). These three cases differ by the flow direction β. Different forms for the dispersion tensor $\mathbf{D}$ can be obtained according to this flow direction and corresponding to the different cases (see Table 2). This allows to study the influence of anisotropy on the numerical results as well. Simulations have been performed up to 200 days with a time step $\delta t = 2$ days. For all cases, an overlap ratio $h/\varepsilon = 0.9$ and a re-griding frequency $N_f = 10$ were selected. To estimate the influence of ε, the $\mathscr{E}r_1$ error has been calculated:

$$\mathscr{E}r_1 = \frac{\sum_{i=1}^{M} |c_a(\mathbf{x}_i) - c_h(\mathbf{x}_i)|^2}{M}, \tag{27}$$

where M is the number of particles with $c_h(\mathbf{x}_i) \geqslant 10^{-6}$ mg/l. On Fig. 1, the logarithm of the $\mathscr{E}r_1$ error has been plotted as a function of the inverse of the smoothing parameter ε for the three cases. The numerical results obtained by Zimmermann et al. have been also plotted. We can then observe that the diffusion velocity method and the PSE method have the same behavior. The errors for all cases can be consistently reduced by decreasing the core radius of the particles. However a lower slope has been obtained with the diffusion velocity method indicating that the convergence is a little bit better for the PSE method. The two methods are basically different since the relative locations of the particle are preserved in a uniform flow in Zimmermann et al. method whereas it is affected by the diffusion velocity in the present case. As it has been observed by Zimmermann et al. for the PSE method, the anisotropy does not have any significant influence on these results. This can be related for a part to the self-adaptivity of the method and for another part to the sphericity of the smoothing function ζ_ε Eq. (3).

Table 2
Forms of the dispersion tensor $\mathbf{D}$

Case	1–3	2–4–6–7	5
$\mathbf{D}$	$\begin{pmatrix} a & 0 \\ 0 & b \end{pmatrix}$	$\begin{pmatrix} a & b \\ b & a \end{pmatrix}$	$\begin{pmatrix} a & b \\ b & c \end{pmatrix}$

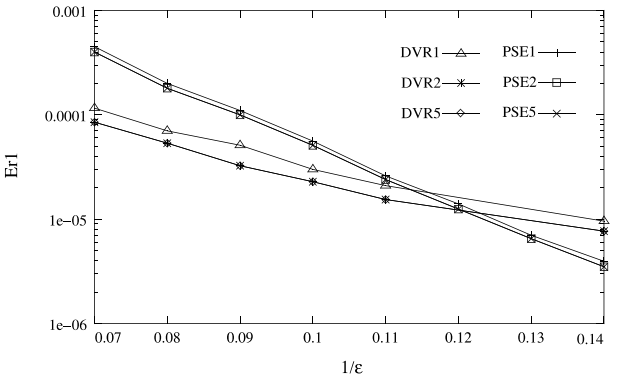

Fig. 1. Logarithm of the $\mathscr{E}r_1$ error with respect to the inverse of the smoothing parameter ε: diffusion velocity method (case 1, DVR1; case 2, DVR2; case 5, DVR5) and particle strength exchange method (case 1, PSE1; case 2, PSE2; case 5, PSE5).

3.3. Time step δt

Following Zimmermann et al. paths, the influence of the time step δt has been investigated. Unlike Zimmermann et al. work, only a second order smoothing function has been used in this work (Eq. (8)). In this section, the three cases denoted 1, 3 and 4 have been considered. The numerical parameters for each case are given in Table 1. The numerical simulations have been performed on 200 days and the smoothing parameter ε has been set to 11 m. The overlap ratio h/ε and the re-griding frequency N_f are respectively equal to 0.9 and 10. Cases 1 and 3 differ only through the values attributed to the longitudinal and transversal dispersivities which are ten times higher for the last case. Case 4 is similar to case 3 for the dispersion characteristics, the flow direction having been set to $\beta = 45°$. For each case, the logarithm of the error $\mathscr{E}r_1$ with respect to the time step δt has been reported and compared to Zimmermann et al. results. Fig. 2 shows that the diffusion velocity method and the PSE method have not the same behaviour for all cases. In case 1, for time steps δt ranging from 5 to 50 days, the $\mathscr{E}r_1$ error with the PSE method remains constant for time steps up to 25 days where it starts to grow slowly. The $\mathscr{E}r_1$ error varies between 5×10^{-5} and 10^{-3}. For the diffusion velocity method, the $\mathscr{E}r_1$ error grows constantly up to 35 days where it seems to reach a plateau. The $\mathscr{E}r_1$ error is then about 2×10^{-2}. For cases 3 and 4, the $\mathscr{E}r_1$ error is constant with the diffusion velocity method for time steps up to 3 days where it starts to grow slowly, reaching respectively

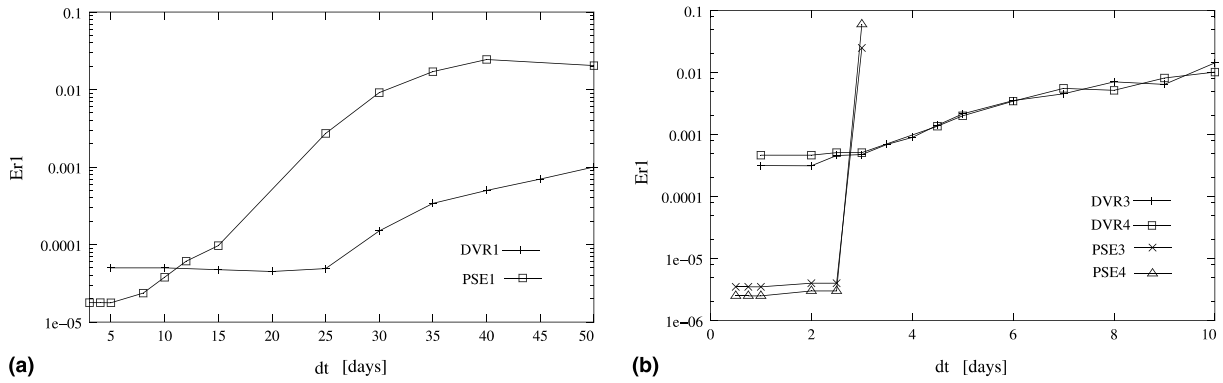

Fig. 2. Logarithm of the $\mathscr{E}r_1$ error with respect to the time step dt: diffusion velocity method (a, case 1: DVR1; b, case 3: DVR3 and case 4: DVR4) and particle strength exchange method (a, case 1: PSE1; b, case 3: PSE3 and case 4: PSE4).

1.43×10^{-2} and 1.02×10^{-2} for a 10 days time step. For the same cases 3 and 4, Zimmermann et al. have shown that the PSE method was stable for time steps up to 2.6 days which correspond to the following stability condition:

$$\delta t \leqslant c \frac{h^2}{D_{xx} + D_{yy}}. \tag{28}$$

This stability condition is not necessary for the diffusion velocity method which was found to be stable for all the tested time steps. It was also observed that the anisotropic dispersion does not have any more effects on the quality of the results. It is important to notice that the regularity of the numerical error as a function of the time step in this particular case does not mean that the method does not suffer any instabilities at all. Such a statement would required to be supported by a rigorous stability analysis which is not available actually. Moreover, it has been observed [8] that an increasing time step will probably results in oscillations, particularly in region with strong gradients or discontinuities. This problem which is partially corrected by the use of a re-gridding procedure hereafter would necessitates more investigations. It is probable that the mathematical analysis of the method would be of great help in this scope.

3.4. Re-griding procedure

In this section, the re-griding procedure has been studied. The analysis of the re-griding influence has been split into three parts. In the first part, the improvement associated to the anti-diffusion step of the re-griding process on the error of the projection step has been checked. In the second part, the behaviour of the re-griding procedure applied to case 2 has been investigated. In the third part, the present re-griding procedure has been compared to the remeshing procedure used in Zimmermann et al. work. For this third part, the case 6 without dispersion has been considered as in Zimmermann et al. work (see Table 1).

First, the re-griding procedure has been tested by performing the same computations with only the projection step and with the full procedure including the anti-diffusion step. The number of re-gridings N_r has been set to different values uniformly distributed within the range $[0, 35]$. The L^2 error $\mathscr{E}r_2$ has been evaluated on a grid as:

$$\mathscr{E}r_2 = \sqrt{\frac{\sum_{i,j}(c_a(\mathbf{x}_n(i,j)) - c_h(\mathbf{x}_n(i,j)))^2}{\sum_{i,j}(c_a(\mathbf{x}_n(i,j)))^2}}, \tag{29}$$

where $c_a(\mathbf{x}_n(i,j))$ is the exact analytical concentration at the fixed grid nodes denoted $\mathbf{x}_n(i,j)$ and $c_h(\mathbf{x}_n(i,j))$ is the numerical concentration at these same points. As regard to the particle distribution, the initial condition of case 1 has been used. On Fig. 3, the logarithm of the $\mathscr{E}r_2$ error with respect to the number of re-gridings N_r has been reported with and without the anti-diffusion step (Eq. (19)). When the re-griding procedure has been used without any anti-diffusion step, the $\mathscr{E}r_2$ error increases constantly with N_r. The effect of the anti-diffusion step is to reduce the order of magnitude of the $\mathscr{E}r_2$ error which is by far lower.

The study of the influence of the re-griding procedure on the numerical results of case 2 is illustrated by 4 different plots:

- The breakthrough curve of the numerical (with and without re-griding procedure) and analytical solutions at point $\mathbf{x}(25, -25)$ (Fig. 4(a)).
- The maximum concentration curve for both numerical (with and without re-griding procedure) and analytical solutions (Fig. 4(b)).
- The logarithm of the $\mathscr{E}r_2$ error with respect to time t (with and without re-griding procedure) (Fig. 5(a)).
- The logarithm of the relative error $\mathscr{E}r_3$ with respect to time t (with and without re-griding procedure) (Fig. 5(b)).

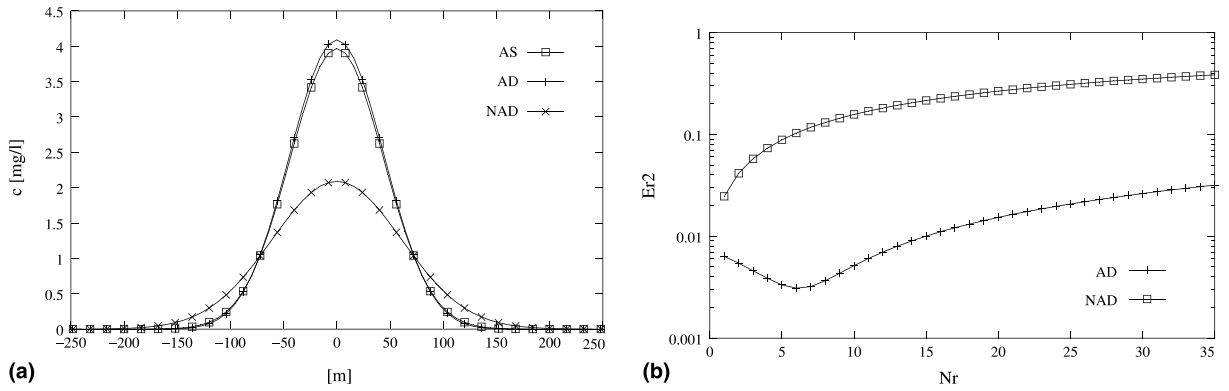

Fig. 3. Concentration curve after 35 re-griding steps (a) (analytical solution: AS, solution with the anti-diffusion step: AD and solution without the anti-diffusion step: NAD) and logarithm of the $\mathscr{E}r_2$ error with respect to the number of re-gridings N_r (b) (solution with the anti-diffusion step: AD and solution without the anti-diffusion step: NAD).

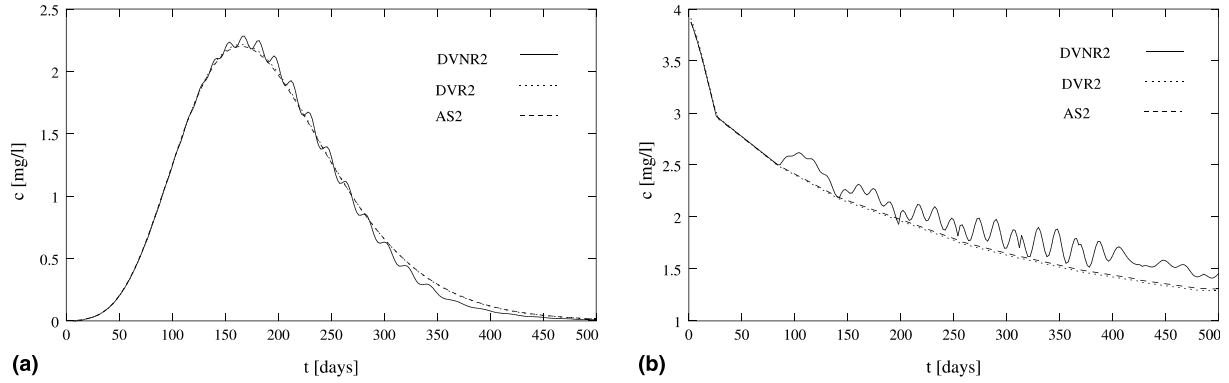

Fig. 4. Breakthrough curve at point $\mathbf{x}(25,-25)$ (a) and maximum concentration curve (b) for case 2: diffusion velocity method without the re-griding procedure (DVNR2), diffusion velocity method with the re-griding procedure (DVR2) and analytical solution (AS2).

Simulations have been performed up to 500 days with a time step $\delta t = 2$ days. The other parameters used are given in Table 1. Note that an overlap ratio $h/\varepsilon = 0.9$ and a smoothing parameter $\varepsilon = 10.0\,\mathrm{m}$ were selected for the simulations.

As in Zimmermann et al. paper, the relative error $\mathscr{E}r_3$ was defined by:

$$\mathscr{E}r_3 = \sqrt{\frac{\left(c_a^{\max} - c_h^{\max}\right)^2}{\left(c_a^{\max}\right)^2}}, \tag{30}$$

where $c_h^{\max}$ and $c_a^{\max}$ are respectively the maximum of the numerical and analytical concentrations. On the breakthrough curve and the maximum concentration curve (see Fig. 4), wiggles are observed for the numerical results without re-griding procedure. This is the result of the difficulty encountered to ensure the overlapping condition with the diffusion velocity method. The re-griding procedure allows to overcome this problem. Looking at the $\mathscr{E}r_2$ error and the $\mathscr{E}r_3$ error (see Fig. 5) gives a better enlightenment of the effect of the re-griding since they are reduced and almost constant for larger time. At time $t = 500$ days, the $\mathscr{E}r_2$ error is about 0.01 with the re-griding process and 0.10 without it. For the $\mathscr{E}r_3$ error, at the same time, we have $\mathscr{E}r_3 \approx 0.015$ with the re-griding and $\mathscr{E}r_3 \approx 0.13$ without it. Numerical tests have shown that a good compromise for the re-

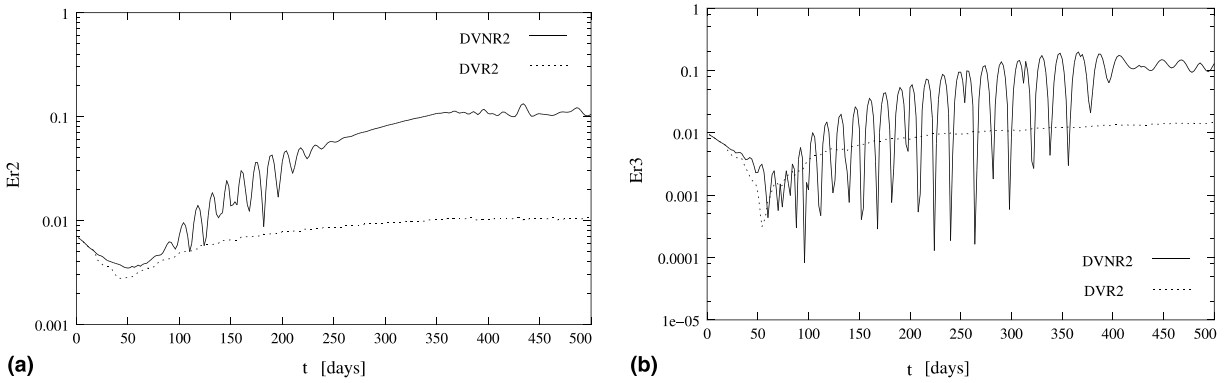

Fig. 5. Logarithm of the $\mathscr{E}r_2$ error with respect to time t (a) and logarithm of the $\mathscr{E}r_3$ error with respect to time t (b) for case 2: diffusion velocity method without the re-griding procedure (DVNR2) and with the re-griding procedure (DVR2).

griding frequency is $N_f = 10$ for this case. However, an increasing of the re-griding frequency N_f will yield a improve accuracy. This point will be detailed in the next section. Eventually, some comparison were made with the re-griding procedure used by Zimmerman et al. This one is based on a in single step with a fourth order projection function [6] applied at every time step, thus $N_f = 1$. The $\mathscr{E}r_3$ error as a function of time has been plotted on Fig. 6 for both methods. The simulations have been performed up 300 days with a time step $\delta t = 10$ days. The others parameters used are those of case 6. The errors have the same order of magnitude for both methods although slightly better results have been obtained using the Cottet–Koumoutsakos procedure.

3.5. Large dispersion ratio

In this section, the contaminant migration with an important ratio of the longitudinal and transversal dispersivities α has been simulated. The aim of these calculations was to explore wether the velocity diffusion method can be efficiently used for anisotropic problems and what its limits can be. The dispersion ratio α is defined by:

$$\alpha = \frac{\alpha_l}{\alpha_t}. \tag{31}$$

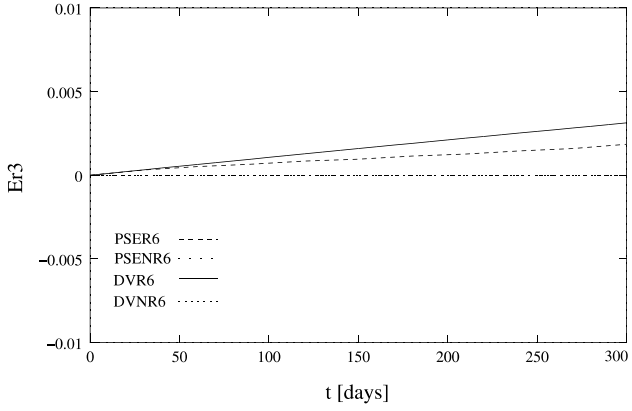

Fig. 6. $\mathscr{E}r_3$ error with respect to time t for case 6: diffusion velocity method without the re-griding procedure (DVNR6) and with the re-griding procedure (DVR6), particle strength exchange method without the re-griding procedure (PSENR6) and with the re-griding procedure (PSER6).

For the numerical simulations with high dispersion ratios ($\alpha = 100$), we have used the case 8 of the Zimmermann et al. paper, noted 7 hereafter. The values of parameters for this case are given in Table 1. Numerical simulations up to 1000 days have been performed with a time step $\delta t = 2$ days. The overlap ratio h/ε and the smoothing parameter ε are respectively fixed to 0.9 and 11.0 m. Different re-griding frequency N_f from 1 to 10 have been tested.

On Fig. 7, the plume of contaminant for both analytical and numerical solutions with the full re-griding procedure has been plotted at times $t = 200$ days, $t = 500$ days and $t = 1000$ days. No oscillations where observed in the surrounding of the plume which seems to indicate that the residual diffusion error which remains after the anti-diffusive step has a positive action, at least in this case. In Fig. 8, we present the

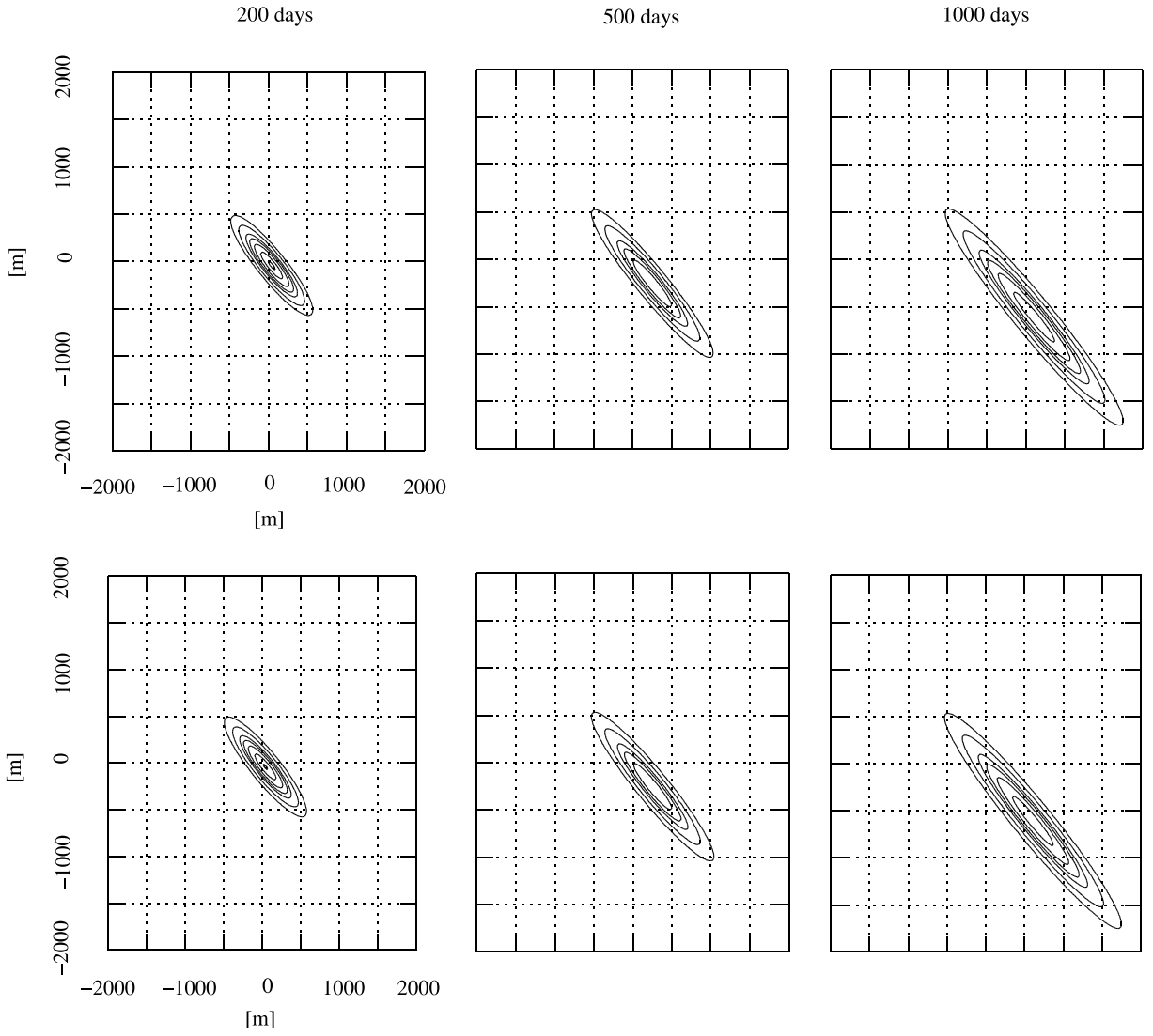

Fig. 7. Comparaison between the analytical solution (bottom) and the numerical solution with the re-griding procedure (top) for case 7 at 200 days, 500 days and 1000 days. The contour lines represent the following concentrations $c = 0.01$, 0.1, 0.5, 1.0, 2.0, 4.0, 6.0, 8.0 mg/l.

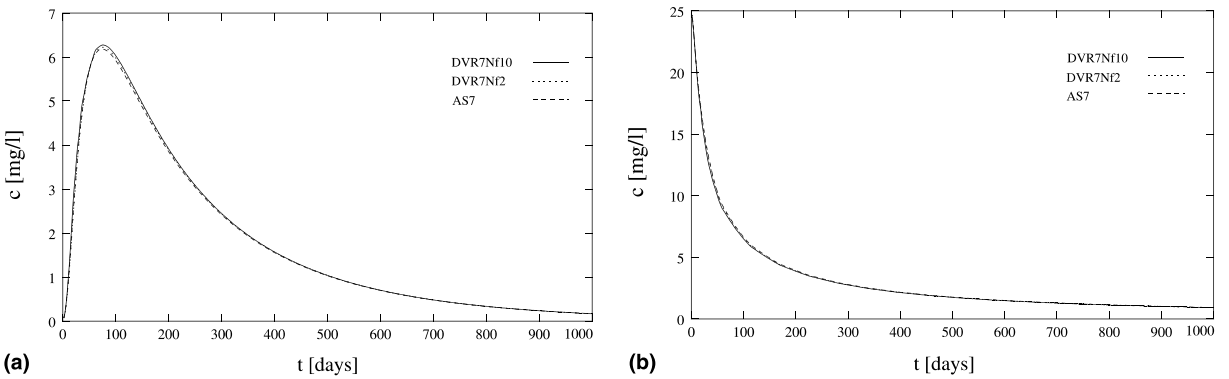

Fig. 8. Breakthrough curve at point $\mathbf{x}(20,-20)$ (a) and maximum concentration curve (b) for case 7: diffusion velocity method with the re-griding frequency $N_f = 2$ (DVR7Nf2) and analytical solution (AS7).

breakthrough curve at point $\mathbf{x}(20,-20)$ and the maximum concentration curve. Two different re-griding frequency, $N_f = 2$ and $N_f = 10$, were used. A better accuracy was achieved with the higher frequency which is consistent with the observations of the previous section.

This is confirmed on Fig. 9 where the $\mathscr{E}r_3$ error with different re-griding frequency has been compared to Zimmermann et al. results. The $\mathscr{E}r_3$ error is always lower than 0.012, ranging from 0.012 for $N_f = 10$ to 0.007 for $N_f = 1$. It is a decreasing function of $N_f = 10$ which is not really a surprise. Note that Zimmermann et al. obtained a $\mathscr{E}r_3$ error of 0.07 with a second order cutoff function and a very comparable 0.006 with a fourth order cutoff function at time $t = 1000$ days.

It was also observed that the error grows more rapidly during the first 50 days, probably to the important relative increasing of the inter-particle distance during this early stage. This problem can be partly cured by using an adaptive re-griding frequency during the early development of the solution in order to satisfy the $h/\varepsilon < 1$ condition after what a constant N_f is to be used. Thanks to the application of the re-griding procedure, the particle number N_p increases during the computation. It has been plotted with respect to time t on Fig. 10. At the end of the simulations, the number of particles N_p ranges from 21,000 for $N_f = 10$ to $N_p \approx 45{,}000$ for the other re-griding frequencies. These number are slightly larger than the 17,000–30,000 particles used by Zimmerman et al. although it is of the same order of magnitude.

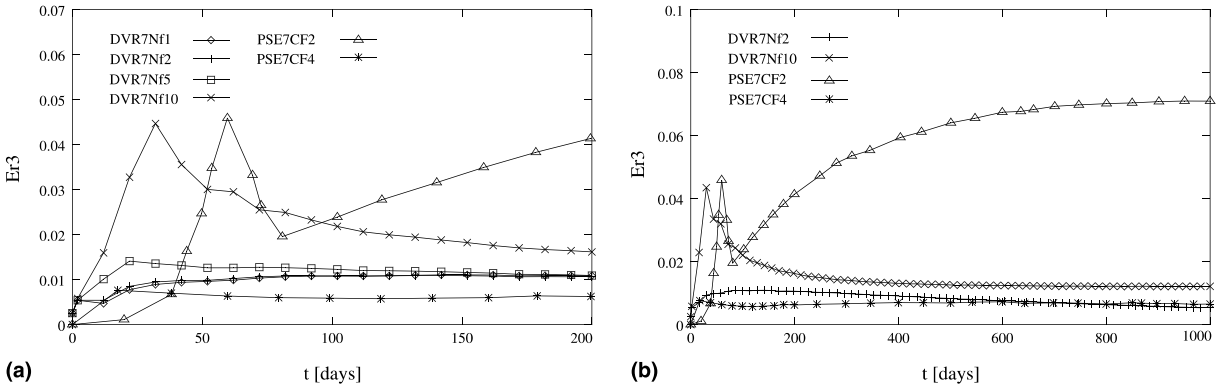

Fig. 9. $\mathscr{E}r_3$ error with respect to time t for 200 days (a) and for 1000 days (b) for case 7: diffusion velocity method with re-griding frequencies $N_f = 1$ (DVR7Nf1), $N_f = 2$ (DVR7Nf2), $N_f = 5$ (DVR7Nf5) and $N_f = 10$ (DVR7Nf10), particle strength exchange method with a second order cutoff function (PSE7CF2) and with a fourth order function (PSE7CF4).

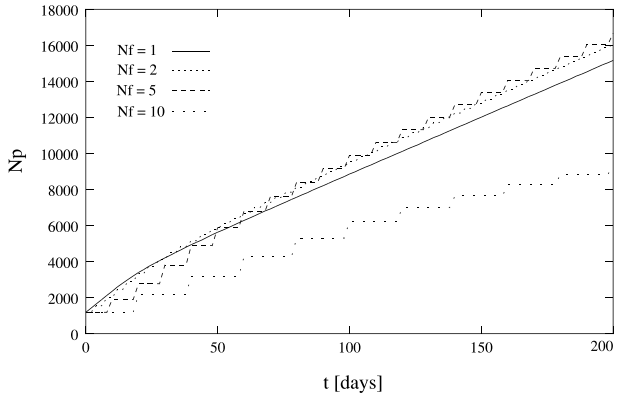

Fig. 10. Particles number N_p used in case 7 with respect to time t with the diffusion velocity method and re-griding frequencies $N_f = 1$, 2, 5 and 10.

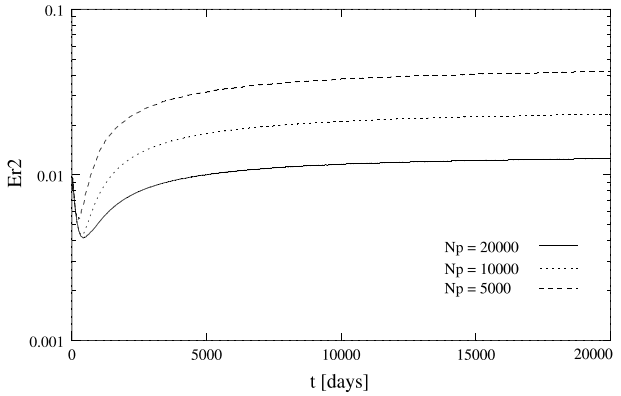

Fig. 11. Logarithm of the $\mathscr{E}r_2$ error with respect to time t for case 7 with limit particles numbers $N_p = 20{,}000$, 10,000 and 5000.

The last test presented in this paper concerns the ability of the method to compute an accurate solution on very long time which is the case of many practical situations. A number of 10,000 time steps was selected with the same 2 days value thus leading to a total duration of the diffusion process of 55 years. The re-griding frequency was $N_f = 5$ and the total number of particles was bounded. Three different cases were performed with $N_p < 5000$, 10,000, 20,000. The satisfaction of the overlapping condition with a fixed number of particles requires an adaptive smoothing parameter. The value of this parameter is computed during the re-griding process from the grid concentration. The logarithm of the $\mathscr{E}r_2$ error with respect to time t has been plotted on Fig. 11. The error at the end of the simulation is roughly proportional to the particles number inverse ranging from 0.042 for 5000 particles to 0.012 for 20,000 particles.

4. Conclusion

The diffusion velocity method was successfully applied to the set of test problems used in Zimmermann et al. work. It was readily found that the extension of the method to anisotropic non-uniform dispersion is by far easier to derive than that of the PSE method. Beside this the PSE results indicate that this method has

better accuracy properties. This is somewhat counterbalanced by the better stability of the present method which does not require the fulfillment of any stability condition, at least within the range of the time step values tested in this work. The method has also been found very sensitive to the fulfillment of the overlapping condition due to the purely advective nature of the equations solved. Therefore, the use of a regriding procedure drastically improve the accuracy. Last, an additional advantage is the ability of the method to automatically satisfy unbounded external conditions [12]. Eventually, the two methods have been found to be able to provide good results for dispersion problems. The choice between the two methods if necessary would rely on the balance between accuracy for the PSE method versus robustness and simplicity for the diffusion velocity method, and may be the personal taste of the user.

References

[1] J. Barnes, P. Hut, A hierachircal $\mathcal{O}(N \log N)$ force-calculation algorithm, Nature 324 (1986) 446–449.
[2] J. Bear, Dynamics of Fluids in Porous Media, Dover, New York, 1972.
[3] J.P. Choquin, S. Huberson, Particles simulation of viscous flow, Comput. Fluids 17 (1989) 397–410.
[4] A.J. Chorin, Numerical study of slightly viscous flow, J. Fluid Mech. 57 (1973) 785–796.
[5] A.J. Chorin, Vortex sheet approximation of boundary layers, J. Comput. Phys. 27 (1978) 428–442.
[6] G.H. Cottet, P. Koumoutsakos, Vortex Methods Theory and Practice, Cambridge University Press, Cambridge, 2000.
[7] P. Degond, S. Mas-Gallic, The weighted particle method for convection–diffusion equations, Part 2: The anisotropic case, Math. Comput. 53 (1989) 509.
[8] P. Degond, F.J. Mustieles, A deterministic approximation of diffusion equations using particles, SIAM J. Sci. Stat. Comput. 11 (1990) 293–310.
[9] D. Fishelov, A new vortex scheme for viscous flows, J. Comput. Phys. 86 (1990) 211–224.
[10] J. Fronteau, P. Combis, A lie-admissible method of integration of Folker–Plank equations with non linear coefficients (exact and numerical solutions), Hadronic J. 7 (1984) 911–930.
[11] L. Greengard, V. Rokhlin, A fast Algoritm for particles simulations, J. Comput. Phys. 73 (1987) 325–348;
, J. Comput. Phys. 73 (325) (1987) 325–348.
[12] S. Huberson, O. Le Maître, E. Rivoalen, Particle simulation of diffusion with non uniform viscosity, ESAIM Proc., vol. 7, 1999, pp. 195–204. Third International Workshop on Vortex – Flows and Related Numerical Methods – http://www.edpsciences.org/articles/proc/Vol.7/index.html.
[13] P.L. Lions, S. Mas-Gallic, Une méthode particulaire déterministe pour des équations diffusives non linéaires, C.R. Acad. Sci. Paris t. 332 (série 1) (2001) 369–376.
[14] A. Jollès, S. Huberson, Correction de l'erreur de projection dans les méthodes particules-maillages, La recherche aérospatiale 4 (1990) 1–6.
[15] G. Lacombe, Analyse d'une équation de vitesse de diffusion, C.R. Acad. Sci. Paris, série I 329 (1999) 383–386.
[16] G. Lacombe, S. Mas-Gallic, Presentation and Analysis of a Diffusion–Velocity Method, ESAIM Proc., vol. 7, 1999, pp. 225–233. Third International Workshop on Vortex – Flows and Related Numerical Methods – http://www.edpsciences.org/articles/proc/Vol.7/index.html.
[17] E. Rivoalen, S. Huberson, Numerical simulation of axisymmetric viscous flows by means of a particle method, J. Comput. Phys. 152 (1999) 1–31.
[18] S. Zimmermann, P. Koumoutsakos, W. Kinzelbach, Simulation of pollutant transport using a particle method, J. Comput. Phys. 173 (2001) 322–347.